Chinese Chemical Letters 32 (2021) 271–276

Contents lists available at ScienceDirect

Chinese Chemical Letters

journal homepage: www.elsevier.com/locate/cclet

Communication

Polyoxygenated anti-inflammatory biscembranoids from the soft coral *Sarcophyton tortuosum* and their stereochemistry

Yufen Li[a,1], Songwei Li[a,b,1], Cristina Cuadrado[c,1], Chenglong Gao[d], Qihao Wu[a], Xiaolu Li[a], Tao Pang[d], Antonio Hernandez Daranas[c,*], Yuewei Guo[a,*], Xuwen Li[a,*]

[a] State Key Laboratory of Drug Research, Shanghai Institute of Materia Medica, Chinese Academy of Sciences, Shanghai 201203, China
[b] School of Chinese Materia Medica, Nanjing University of Chinese Medicine, Nanjing 210023, China
[c] Instituto de Productos Naturales y Agrobiologi'a, Consejo Superior de Investigaciones Científicas (IPNA-CSIC), La Laguna 38206, Spain
[d] Jiangsu Key Laboratory of Drug Screening, State Key Laboratory of Natural Medicines, Jiangsu Key Laboratory of Drug Discovery for Metabolic Diseases, China Pharmaceutical University, Nanjing, 210009 China

ARTICLE INFO

Article history:
Received 25 September 2020
Received in revised form 27 October 2020
Accepted 16 November 2020
Available online 23 November 2020

Keywords:
Soft coral
Sarcophyton tortuosum
Biscembranoid
Stereochemistry
Anti-inflammatory

ABSTRACT

Five novel biscembranoids, ximaolides H–L (**1**–**5**), along with four known related compounds (**6**–**9**) were isolated from the Hainan soft coral *Sarcophyton tortuosum*. The structures of the new compounds were determined by extensive spectroscopic analysis, quantum chemical calculations, and/or by comparing their CD spectra with those of the known compounds. Compounds **1** and **2** are the first examples of biscembranoids bearing a 1,35-bridged lactone moiety, **4** is the first biscembranoid comprising an uncommon oxetane ring, and **5** represents the first 36-peroxyl biscembranoid. Ximaolides I (**2**), K (**4**) and F (**9**) exhibited interesting anti-inflammatory activity by the inhibition of LPS-induced TNF-α protein release in RAW264.7 macrophages.

Soft corals of the genus *Sarcophyton* (family Alcyoniidae), chemically and biologically investigated over decades, were regarded as rich sources of structurally diverse and biologically active terpenoids, *e.g.*, cembranoids [1]. Although cembranoids were frequently encountered in marine Cnidaria, dimeric cembranoids (biscembranoids) were rare, with only approximate 70 examples been found in Nature, mostly in *Sarcophyton* soft corals [1–6]. Depending on the dimerization patterns of the Diels-Alder reaction over monomeric cembranoids, biscembranoids mainly comprise three types, including ximaolides [7,8], bisglaucumlides [9] and bislatumlides [10]. A wide range of biological activities, such as cytotoxic, antimicrobial and anti-inflammatory effects, have been reported for these biscembranoids [11]. South China Sea breeds abundant marine life, including over 40 identified species of *Sarcophyton* soft corals, of which nearly 20 species were chemically investigated and about half of them were reported by our group. In fact, our group has long been engaged in the chemical and biological studies on marine invertebrates from South China Sea, and numerous complex and bioactive terpenoids were isolated and structurally determined [12,13,14a,b,15–17]. In particular, over one third of the natural biscembranoids have been discovered by our group, such as ximaolides A–G [7,8], and bislatumlides C–F [10], which were isolated from *S. tortusum* and *S. latum* of previous collections.

In order to expand the structural diversity and pharmacological applications of biscembranoids from *S. tortusum*, as well as to deal with the challenging configurational problems of several complex molecules, the title animals were recollected from Yalong Bay, Hainan, China. A systematic chemical investigation has led to the isolation and structural determination of five novel biscembranoids, ximaolides H-L (**1**–**5**), together with four known related ones (**6**–**9**) (Fig. 1). Herein, we report the isolation, structural elucidation, and biological activity evaluation of the isolated metabolites.

The frozen title animals (dry weight 100 g) were cut into pieces and exhaustively extracted with acetone. The Et_2O-soluble portion of the acetone extract was repeatedly column chromatographed over silica gel, Sephadex LH-20, and RP-HPLC to yield nine pure compounds **1**–**9**, respectively. The structures of the known compounds were readily identified as ximaolide A (**6**) [7], methyl sartortuoate (**7**) [18], methyl tortuoate B (**8**) [19] and ximaolide F (**9**) [8], respectively, by direct comparison of their NMR data and CD spectra with those reported in the literature.

* Corresponding authors.
E-mail addresses: adaranas@ull.edu.es (A.H. Daranas), ywguo@simm.ac.cn (Y. Guo), xwli@simm.ac.cn (X. Li).
[1] These authors are contributed equally to this work.

https://doi.org/10.1016/j.cclet.2020.11.037
1001-8417/

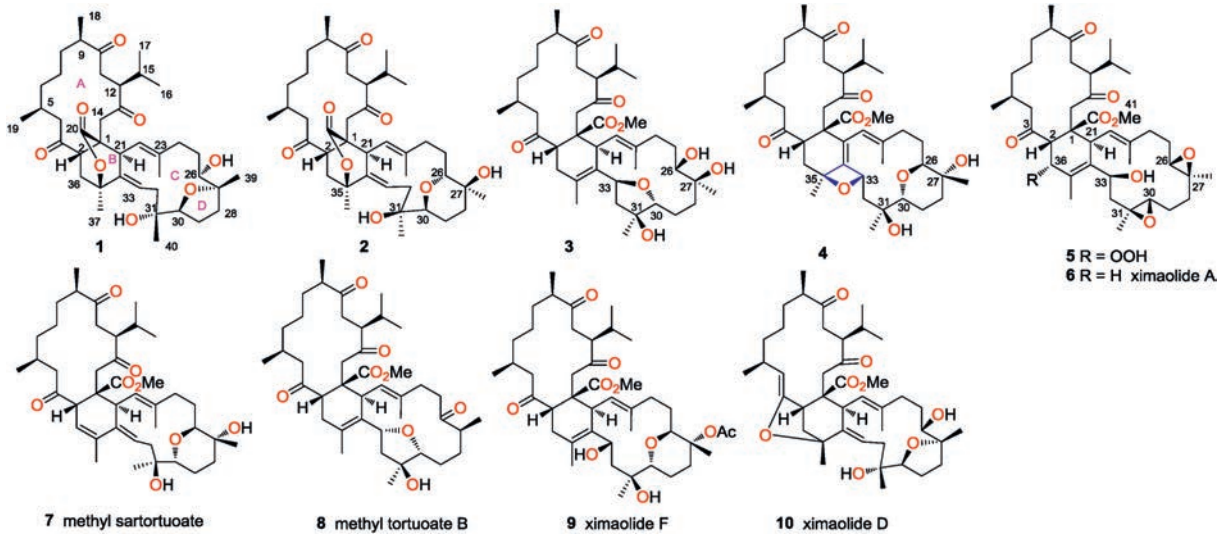

Fig. 1. Structures of compounds **1** – **10**.

Ximaolide H (**1**) was obtained as a white amorphous powder. Its molecular formula was deduced to be $C_{40}H_{60}O_8$ by HREI-MS from the molecular ion peak at *m/z* 668.4295 $[M]^+$ (calcd. 668.4288), indicating eleven degrees of unsaturation. The analysis of ^{13}C NMR data, DEPT and HSQC spectra of **1** revealed 40 carbon signals, including three ketone carbonyl groups (δ_C 214.5, 213.6, 209.3), an ester carbonyl group (δ_C 173.6), four olefinic carbons (δ_C 139.4, 138.8, 121.9, 121.7), five oxygenated carbons (δ_C 87.1, 83.9, 82.5, 73.8, 71.9), and eight methyls (δ_C 22.5, 22.3, 22.2, 21.0, 20.3, 19.4, 17.4, 17.3) (Table 1). Four carbonyls and two double bonds accounted for six degrees of unsaturation, indicating that **1** contained a pentacyclic system. These NMR data were reminiscent of those of the co-isolated known compounds **6**–**9**, suggesting that ximaolide H (**1**) possesses a biscembranoid skeleton. In particular, the similar NMR signals from C-3 to C-19 between **1** and **6**–**9** indicated that they should share a common ring A. Further literature survey and careful data comparison indicated that **1** should comprise the same rings C and D as ximaolide D (**10**) [7], a biscembranoid previously isolated by our group from the Hainan soft coral *S. tortuosum*, since they showed very similar NMR signals from C-21 to C-34. Therefore, the remaining task to identify the planar structure of compound **1** was the substitution patterns on ring B. The only significant differences between **1** and ximaolide D on ring B were the lack of a carbomethoxy group at C-1 in **1** and the downfield shift of C-35 from δ_C 76.9 in ximaolide D to 82.5 in **1**, suggesting that the methyl ester at the C-1 position of ximaolide D was replaced by an 135-bridged lactone moiety on ring B of **1**. The proposed planar structure of **1** was further confirmed by detailed analysis of its 2D NMR spectra, including ^1H-^1H COSY and HMBC experiments, as shown in Fig. 2. In particular, the key HMBC correlations from H_2-14 (δ_H 3.20, 3.02) and H-21 (δ_H 4.30) to C-20 (δ_C 173.6); from H-21, H-33 (δ_H 5.35), and H_2-36 to C-35 (δ_C 82.5), supported the linkage position of the 135-bridged lactone.

The *E* geometry of Δ3334 was determined by the clear NOE correlation between H-33 and H_3-37 (δ_H 1.52), whereas the absence of the NOE cross peak between H-22 (δ_H 4.55) and H_3-38 (δ_H 1.91) and the clear NOE relationship between H-22 and H_2-24 (δ_H 2.17) (Fig. 2) indicated the *E* geometry of $\Delta^{22,23}$. According to our previous research, the three isolated carbonyl groups in ring A of ximaolides A – C and E – G [7,8,20], due to the n-π^* transitions, resulted in a positive Cotton effect at 282 nm in its CD spectrum

Table 1
The ^{13}C NMR data of compounds **1**-**5** in $CDCl_3$.[a]

No.	δ_C, mult				
	1	**2**	**3**	**4**	**5**
1	46.7, s	47.0, s	49.5, s	52.2, s	52.8, s
2	43.8, d	44.0 d	43.0, d	47.4, d	49.7, d
3	209.3, s	209.7, s	213.7, s	210.7, s	213.2, s
4	49.2, t	49.3, t	54.2, t	52.6, t	54.0, t
5	28.5, d	28.7, d	27.6, d	27.9, d	27.6, d
6	36.9, t	37.1, t	37.5, t	38.0, t	37.4, t
7	25.5, t	25.6, t	25.5, t	26.3, t	25.8, t
8	34.0, t	34.0, t	33.9, t	34.9, t	34.3, t
9	48.3, d	48.4, d	47.6, d	49.2, d	48.6, d
10	214.5, s	214.5, s	214.1, s	213.7, s	213.9, s
11	36.5, t	36.6, t	31.6, t	31.6, t	31.3, t
12	51.5, d	51.6, d	52.0, d	51.0, d	50.6, d
13	213.6, s	213.5, s	208.6, s	209.7, s	209.7, s
14	42.8, t	43.0 t	45.2, t	43.3, t	47.5, t
15	29.5, d	29.6 d	29.1, d	29.3, d	29.0, d
16	19.4, q	19.4, q	17.7, q	18.0, q	17.8, q
17	21.0, q	21.0, q	21.5, q	21.5, q	21.3, q
18	17.4, q	17.4, q	17.6, q	17.9, q	17.7, q
19	22.2, q	22.3, q	22.4, q	22.6, q	22.0, q
20	173.6, s	173.5, s	174.7, s	173.0, s	174.2, s
21	40.7, d	39.6, d	51.9, d	131.7, s	42.9, d
22	121.7, d	122.2, d	126.2, d	123.0, d	125.8, d
23	139.4, s	139.0, s	135.4, s	137.3, s	134.4, s
24	35.5, t	31.8, t	35.9, t	39.8, t	36.0 t
25	28.6, t	26.3, t	23.3, t	21.4, t	26.4, t
26	71.9, d	86.1, d	67.9, d	87.7, d	61.6, d
27	83.9, s	69.7, s	74.9, s	69.6, s	58.8, s
28	36.3, t	30.7, t	36.7, t	31.4, t	35.9, t
29	26.3, t	20.2, t	20.5, t	20.1, t	23.4, t
30	87.1, d	68.7 d	92.1, d	69.1, d	61.9, d
31	73.8, s	74.1, s	81.3, s	74.6, s	60.6, s
32	33.7, t	37.4, t	48.4, t	43.9, t	40.4, t
33	121.9, d	120.5, d	79.7, d	72.3, d	65.7, d
34	138.8, s	141.2, s	127.2, s	141.0, s	140.3, s
35	82.5, s	82.8, s	131.6, s	85.1, s	128.3, s
36	38.3, t	38.4, t	33.9, t	34.1, d	86.6, d
37	22.3, q	22.5	19.2, q	25.1, q	17.6, q
38	17.3, q	20.6	14.6, q	17.0, q	17.9, q
39	20.3, q	25.6	23.5, q	25.8, q	16.0, q
40	22.5, q	24.1	25.6, q	23.3, q	18.1, q
41			51.4	51.7, q	51.4, q

[a] Recorded at 125 MHz. Assignments were deduced by analysis of 1D and 2D NMR spectra.

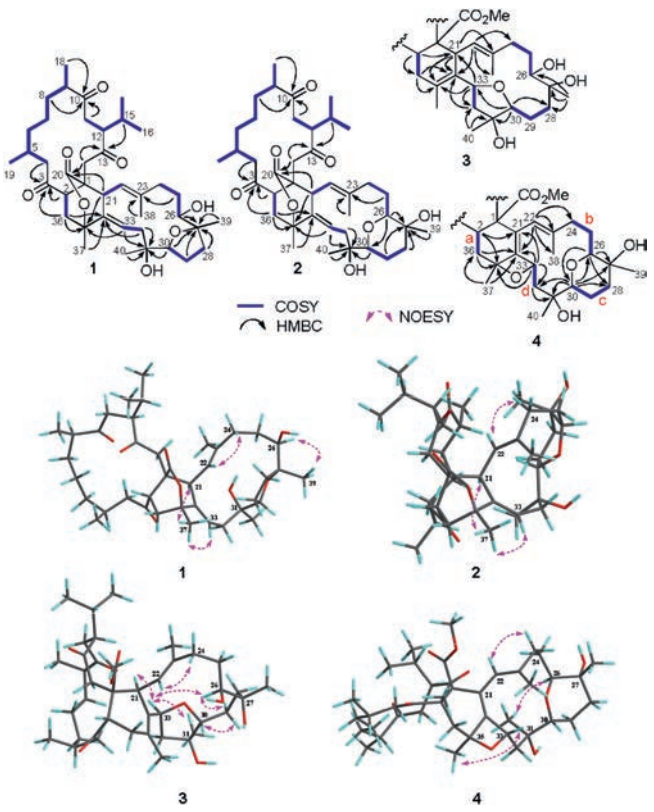

Fig. 2. ^{1}H-^{1}H COSY, key HMBC and NOESY correlations of compounds **1** – **4**.

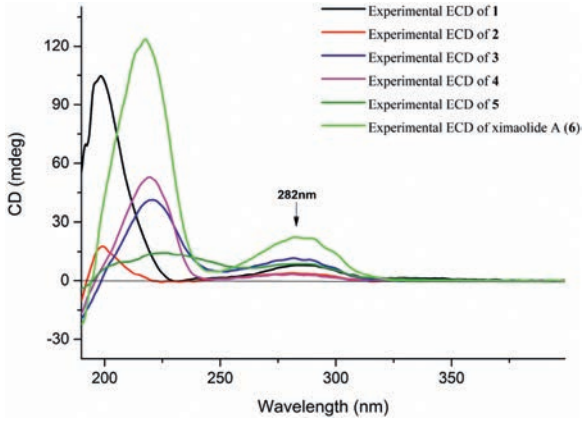

Fig. 3. Experimental ECD spectra of **1** – **6**.

(Fig. 3), which further influenced the stereochemistry of the adjacent chiral carbons C-1, C-2, C-5, C-9, C-12 and C-21.

Therefore, the ACs of C-1, C-2, C-5, C-9, C-12, and C-21 in ximaolide H (**1**) were determined by showing the same positive cotton effect at 282 nm in its CD spectrum as those of ximaolides A, D and F, to be 1*S*, 2*S*, 5*S*, 9*R*, 12*S*, 21*S* (Fig. 3). The configuration of chiral center C-35 was assigned to be *S* by the obvious NOE relationship between H-21 and H_3-37. The major difficulty was to connect the relative configuration of the chiral centers of rings C/D with the remote position C-35. This problem has been tackled by using *J*-based conformational analysis and NOE analysis. The scarcity of informative NOE correlations led us to find feasible alternatives for structural determination. Computational prediction of NMR data is clearly becoming a fast and reliable approach for structure elucidation of natural products [21]. Therefore, the relative configuration of **1** was further deduced by quantum mechanics calculations of its NMR data (QM-NMR). First, conformational searches on the 32 possible candidate diastereoisomers (Fig. S43 in Supporting information) at the Merck Molecular Force Field (MMFF) as implemented in the Macromodel software were performed. All structures found within an energy window of 21 kJ/mol were saved, using an RMSD = 1.0 A. Next, geometrical optimization followed by NMR calculations at the PCM/mPW1PW91/6−31+G**//B3LYP/6−31G* level of theory was done, the most stable conformation by DFT calculations of compound **1** were shown in Fig. 4. NMR shielding constants were calculated using the GIAO approach [22] and were averaged over the Boltzmann distribution estimated for each stereoisomer. Finally, the computed and experimental data were correlated and their corresponding DP4+ probabilities were estimated. As a result, it turned out that the experimental NMR data of compound **1** gave the best match for isomer 1*S**, 2*S**, 5*S**, 9*R**, 12*S**, 21*S**, 26*R**, 27*R**, 30*S**, 31*R**, 35*S** with 99% probability. The selected stereoisomer showed linear correlation coefficients (R^2) of 0.999 and 0.981 (Fig. 5) and CMAE (corrected mean absolute error) values of 1.8 and 0.12 ppm (Table S1 in Supporting information), for carbon and proton data, respectively. Thus, the AC of compound **1** was determined as 1*S*, 2*S*, 5*S*, 9*R*, 12*S*, 21*S*, 26*R*, 27*R*, 30*S*, 31*R*, 35*S*.

Compound **2**, named ximaolide I, was also obtained as white powder. Its HRMS (ESI-TOF) *m/z*: $[M + Na]^+$ calcd. for $C_{40}H_{60}O_8Na$ 691.4186; Found 691.4184, revealed the molecular formula of $C_{40}H_{60}O_8$, which is the same as that of **1**, suggesting that they are isomers. Its ^{1}H and ^{13}C NMR data (Tables 1 and 2) were also similar to those of compound **1**, especially those in rings A and B, indicating the same biscembranoid skeleton with the same ring A and 135-bridged lactone in ring B. The major differences between these two compounds were found to be in the NMR signals from C-25 to C-30, suggesting that the tetrahydrofuran ring of **1** was replaced by a tetrahydropyran ring D in **2**, the same as that of methyl sartortuoate (**7**) [18], with the clear ^{1}H-^{1}H COSY and HMBC correlations as shown in Fig. 2. The *E* geometry of $\Delta^{22,23}$ and $\Delta^{33,34}$, and the configurations of the chiral centers in rings A – C of **2** were deduced to be the same as those of **1** by NOESY experiments (Fig. 2) and by the same positive Cotton effects of their CD spectra (Fig. 3). The configurations of the chiral centers on rings C and D were also determined by the QM-NMR due to the lack of informative NOE relationships. Again, making use of a QM-NMR approach, 32 relative isomers (Fig. S44 in Supporting information) of **2** were built and conformational searches followed by DFT optimization (Fig. 4) and calculation of their NMR parameters were undertaken. The candidate structure with a relative configuration 1*S**, 2*S**, 5*S**, 9*R**, 12*S**, 21*S**, 26*R**, 27*S**, 30*S**, 31*S**, 35*S** gave a best match

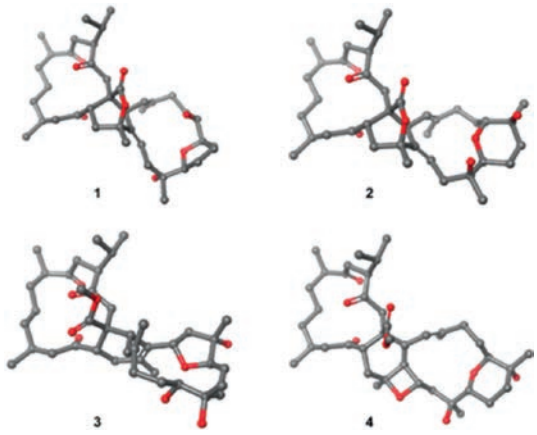

Fig. 4. Most stable conformations by DFT calculations of compounds **1** – **4**.

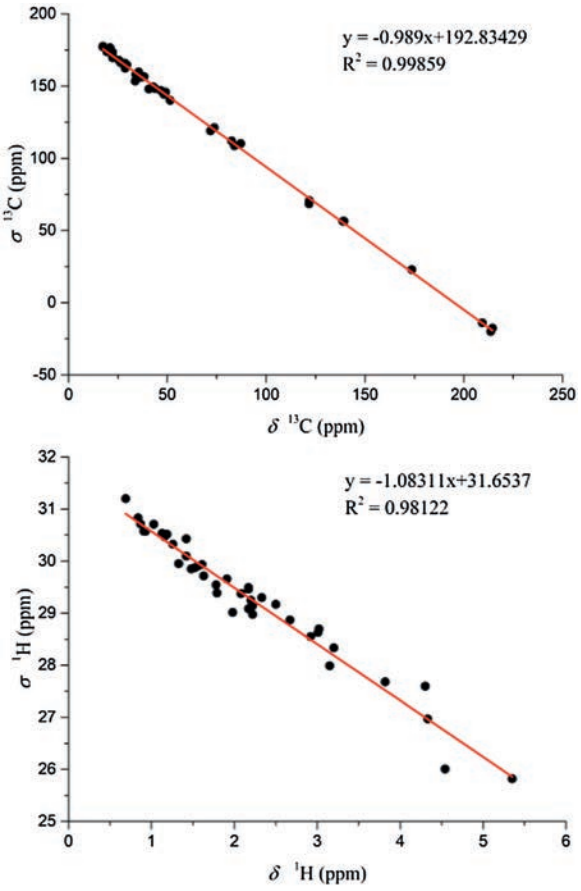

Fig. 5. Correlation plots between $^{13}C/^{1}H$ isotropic magnetic shielding values (σ) computed at the PCM/mPW1PW91/6-31+G** level of theory and experimental $^{13}C/^{1}H$ chemical shifts (δ) for compound **1**.

between experimental and computed data with 99% probability (CMAE of 2.1 and 0.20 ppm).

Based on the above evidence and on biogenetic considerations, the absolute stereochemistry of compound **2** was determined as 1*S*, 2*S*, 5*S*, 9*R*, 12*S*, 21*S*, 26*S*, 27*R*, 30*R*, 31*S*, 35*S*.

Ximaolide J (**3**) was obtained as white powder. Its HREI-MS at *m/z* 700.4555 $[M]^+$ (calcd. for $C_{41}H_{64}O_9$, 700.4550) revealed the molecular formula of $C_{41}H_{64}O_9$, with ten degrees of unsaturation. The ^1H and ^{13}C NMR data (Tables 1 and 2) indicated the presence of a methyl ester [δ_C 174.7 (C), 51.4 (CH_3) and δ_H 3.52 (3H, s)], three ketone carbonyls (δ_C 213.7, 214.1, 208.6), one tri-substituted double bond [$\delta_{C/H}$ 126.2/4.94 (CH), 135.4 (C)] and one tetra-substituted double bond [δ_C 127.2 (C), 131.6 (C)], five oxygenated carbons [$\delta_{C/H}$ 74.9 (C), 81.3 (C), 67.9/3.14 (CH), 79.7/3.93(CH), 92.1/3.99(CH)], and eight methyl groups ($\delta_{C/H}$ 17.7/0.70, 21.5/1.01, 17.6/1.12, 22.4/0.85, 19.2/1.89, 14.6/1.59, 23.5/1.14, 25.6/1.39). All the above data, together with the 2D NMR analysis (Fig. 2), suggested that compound **3** is a biscembranoid, with a structure similar to the co-isolated methyl tortuoate B (**8**) [19]. The main differences between these two compounds occurred on C-26 and C-27. In particular, the secondary hydroxyl at C-26 ($\delta_{C/H}$ 67.9/3.14) and the tertiary hydroxyl at C-27 (δ_C 74.9) of **3** replaced the carbonyl at C-26 (δ_C 215.9) and the methine at C-27 ($\delta_{C/H}$ 49.0/2.37) of **8**. The stereochemistry on rings A and B was determined to be the same as the co-isolated **7**–**9** by the similar positive Cotton effects at 282 nm in their CD spectra. The *E* geometry of $\Delta^{22,23}$ was also deduced by the absence of the NOE cross peaks between H-22 (δ_H 4.94) and H_3-38 (δ_H 1.59), and the clear NOE correlation of H-22 and H_2-24 (δ_H 2.29, 2.12). Furthermore, the clear NOE correlations of H-21 (δ_H 2.61) and H-33 (δ_H 3.93), H-33 and H-26 (δ_H 3.14), H-33 and H_3-40 (δ_H 1.39) determined the relative configuration at C-21, C-26, C-31, and C-33 as 21*S**, 26*S**, 31*S**, 33*S**, while the configuration at C-27 and C-30 was uncertain because of lacking of key NOE signals. Thus, the whole relative configuration of **3** was also elucidated *via* QM-NMR calculations, using the same protocol used for **1** and **2**. 64 candidate diasteroisomers (Fig. S45 in Supporting information) were studied and this time the calculations gave a best match for isomer 1*S**, 2*S**, 5*S**, 9*R**, 12*S**, 21*S**, 26*S**, 27*S**, 30*R**, 31*S**, 33*S** with more than 99% probability (Fig. 4). CMAE values of 1.9 and 0.16 ppm for carbon and proton data, respectively, were obtained.

Based on these evidences and on biogenetic considerations, the absolute configuration of compound **3** was assigned as 1*S*, 2*S*, 5*S*, 9*R*, 12*S*, 21*S*, 26*S*, 27*S*, 30*R*, 31*S*, 33*S* as shown in Fig. 1.

The molecular formular of ximaolide K (**4**) was deduced as $C_{41}H_{62}O_9$ by HREI-MS at *m/z* 698.4401 $[M]^+$, with eleven degrees of unsaturation. The ^1H and ^{13}C NMR spectra (Tables 1 and 2), as well as an HSQC experiment, indicated the presence of a methyl ester [δ_C 173.0 (C), 51.7 (CH_3) and δ_H 3.48 (3H, s)], three ketone carbonyl groups (δ_C 210.7, 213.7, 209.7), one tri-substituted double bond [$\delta_{C/H}$ 123.0/5.63 (CH), 137.3 (C)] and one tetra-substituted double bond [δ_C 131.7 (C), 141.0 (C)], six oxygenated carbons [$\delta_{C/H}$ 87.7/3.58 (CH), 69.6 (C), 74.6 (C), 69.1/3.55 (CH), 72.3/4.77 (CH), 85.1 (C)], and eight methyl groups ($\delta_{C/H}$ 18.0/0.74, 21.5/0.98, 17.9/1.11, 22.6/0.87, 25.1/1.59, 17.0/1.56, 25.8/1.10, 23.3/1.18). All the above signals indicated that compound **4** is also a biscembranoid, with the same ring A as the other co-isolated compounds. Four carbonyls and two double bonds accounted for six degrees of unsaturation, thus the remaining five degrees should be ascribed to a pentacyclic ring system. The ^1H-^1H COSY correlations of H-2 (δ_H 3.86)/H_2-36 (δ_H 2.57, 1.69), H_2-24 (δ_H 2.32, 2.18)/H_2-25 (δ_H 1.89, 1.47)/H-26 (δ_H 3.58), H_2-28 (δ_H 1.93, 1.56)/H_2-29 (δ_H 1.75)/H-30 (δ_H 3.55) and H_2-32 (δ_H 2.03, 1.94)/H-33 (δ_H 4.77) disclosed the proton connectivity for four structural fragments **a**–**d** (Fig. 2). Fragment **a**, along with the HMBC correlations from H-2 to C-21 (δ_C 131.7)/C-35 (δ_C 85.1), H_2-36 to C-34 (δ_C 141.0)/C-35 (δ_C 85.1), H_3-37 (δ_H 1.59) to C-34/C-36 (δ_C 34.1), constituted the six membered ring B, with the tetra-substituted double bond located at $\Delta^{21,34}$. Fragments **b**–**d**, together with the HMBC correlations from H-22 (δ_H 5.63) to C-23 (δ_C 137.3)/C-24 (δ_C 39.8)/C-34/C-38 (δ_C 17.0), H-26 to C-27 (δ_C 69.6)/C-28 (δ_C 31.4), H-30 to C-28/C-31 (δ_C 74.6)/C-32 (δ_C 43.9), H_2-32 to C-31, H-33 to C-21/C-32/C-34/C-35, constructed the 14-membered cembrane ring C, with the location of the trisubstituted double bond at $\Delta^{22,23}$. The biscembranoid skeleton of **4** was then set up, and the remaining two rings must be attributed to two cyclic ethers. The first cyclic ether was deduced to be a tetrahydropyran ring D, connecting C-26 and C-30, since the HMBC correlations from H-26 to C-30 and from H-30 to C-26 have been both observed (Fig. 2). The extremely similar ^{13}C NMR data of C-26/C-27/C-30/C-31 (87.7/69.6/69.1/74.6) with those of the co-occurring compounds **7** and **9**, not only confirmed the presence of the tetrahydropyran ring D, but also indicated that the two hydroxyls should be located at C-27 and C-31. Therefore, the last cyclic ether ring must be constructed by a connection of C-33 and C-35, forming an oxetane ring. Finally, the planar structure of compound **4** was determined as shown in Fig. 1. The relative configuration of **4** was assigned by NOESY correlations and by comparison with the co-isolated compounds **7** and **9** which contain the same tetrahydropyran ring. The relative configuration of chiral centers C-26, C-33 and C-35 were determined to be 26*S**, 33*S**, 35*S** by the distinct NOE correlations of H-26 (δ_H 3.58) and H-33 (δ_H 4.77), H-33 and H_3-37 (δ_H 1.59). The whole relative configuration of **4** was further elucidated *via* QM-NMR calculations, using the DP4+ protocol as used for **1**–**3**. This time the calculations gave a best match for isomer 1*S**, 2*S**, 5*S**, 9*R**, 12*S**, 26*S**, 27*R**, 30*R**, 31*S**, 33*S**, 35*S** with 80% probability (Figs. 4 and

Table 2
The ^{1}H NMR data of compound **1** – **5** in $CDCl_3$.[a]

No.	δ_H, mult (*J* in Hz)				
	1	**2**	**3**	**4**	**5**
2	4.33, dd (13.4, 5.4)	4.30, dd (13.5, 5.5)	3.40, dd (10.7, 7.1)	3.87, dd (11.7, 3.4)	4.20, d (4.5)
4	2.22, m	2.20, m	3.22, dd (19.9, 10.5)	2.78, dd (19.3, 10.1)	3.15, dd (20.1, 10.1)
	2.22, m	2.19, m	2.38, dd (19.9, 1.9)	2.42, m	2.62, dd (20.1, 2.0)
5	2.08, m	2.07, m	1.78, m	1.82, m	1.79, m
6	1.26, m	1.25, m	1.07, m	1.10, m	1.00, m
	0.84, m	0.85, m	1.07, m	1.01, m	1.00, m
7	0.69, m	0.68, m	1.30, m	0.95, m	1.04, m
	0.93, m	0.92, m	1.16, m	1.22, m	1.27, m
8	1.42, m	1.41, m	1.48, m	1.49, m	1.50, m
	1.42, m	1.41, m	1.55, m	1.49, m	1.48, m
9	2.33, ddd (10.2, 7.3, 5.1)	2.31, m	2.56, m	2.36, m	2.44, m
11	2.92, dd (17.6, 11.5)	2.91, dd (17.4, 11.5)	2.96, dd (17.2, 9.9)	2.97, dd (17.4, 10.7)	2.97, d (3.4)
	2.20, m	2.12, dd (17.4, 1.6)	1.87, m	1.68, m	1.90, m
12	3.01, m	2.99, m	3.08, m	3.06, m	3.06, m
14	3.02, d (19.6)	3.12, d (19.6)	2.54, d (18.3)	3.28 d (19.1)	3.02, 2H, m
	3.20, d (19.6)	3.01, d (19.6)	3.04, d (18.3)	3.10 d (19.1)	
15	1.98, m	1.96, m	2.27, m	2.18, m	2.14, m
16	0.91 d (6.8)	0.90 d (6.8)	0.71, d (6.8)	0.74 d (6.8)	0.68, d (6.8)
17	1.03, d (6.8)	1.02, d (6.8)	1.02, d (6.8)	0.98 d (6.8)	0.95, d (6.8)
18	1.13, d (7.0)	1.12, d (7.0)	1.12 d (7.1)	1.11, d (7.0)	1.11, d (7.0)
19	0.87, d (6.9)	0.86, d (6.9)	0.85, d (7.0)	0.87, d (7.0)	0.86, d (7.0)
21	4.30, d (11.2)	4.40, ddd (11.2, 2.1, 2.1)	2.61, d (10.7)		3.49, d (11.0)
22	4.54, brd (10.8)	4.65, d (11.2)	4.94 d (10.6)	5.63, s	5.59, d (10.8)
24	2.17, m	2.17, m	2.29, m	2.32, m	2.25, dd (16.4, 8.3)
	2.17, m	2.17, m	2.12, m	2.18, m	2.05, m
25	1.33, m	1.83, m	1.43, m	1.89, m	2.10, m
	1.78, m	1.45, m	1.69, m	1.47, m	1.49, m
26	3.15, d (9.1)	3.47, d (10.7)	3.14, dd (12.1, 2.1)	3.58, m	2.95, dd (8.7, 5.7)
28	2.17, m	1.58, dd (13.4, 5.6)	1.70, m	1.93, m	2.04, m
	1.55, m	1.52, m	1.78, m	1.56, m	2.04, m
29	1.63, m	1.62, m	1.52, m	1.75, m	1.40, m
	1.48, m	1.47, m	1.44, m	1.75, m	1.67, m
30	3.82, dd (11.2, 4.3)	3.25, brd (11.6)	3.99, dd (12.3, 1.7)	3.55, m	2.35, dd (9.2, 4.3)
32	1.79, m	1.79, m	2.24, m	1.94, m	1.89, m
	2.67, dd (17.4, 8.3)	2.47, t (13.4)	2.24, m	2.03, brd (14.7)	1.80, m
33	5.35, ddd (8.1, 2.5, 2.5)	5.59, ddd (11.7, 2.7, 2.7)	3.93, t (8.9)	4.77, d (11.1)	5.02 dd (11.3, 2.7)
36	2.50, t, (13.6)	2.50, m	1.92, m	2.57, dd (14.0, 11.7)	4.68 d (4.5)
	1.61, dd (13.6, 5.6)	1.59, m	2.50, m	1.69, m	
37	1.52, s	1.55, s	1,89, s	1.59, s	1.91 s
38	1.91, d (1.3)	1.96, s	1.59, s	1.56, s	1.61, s
39	1.16, s	1.08, s	1.14, s	1.10, s	1.25, s
40	1.19, s	1.18, s	1.39, s	1.18, s	1.30, s
41			3.52, s	3.48, s	3.49, s
OOH					8.76, s

[a] Recorded at 500 MHz. Assignments were deduced by analysis of 1D and 2D NMR spectra.

Fig. S50 in Supporting information). CMAE values of 2.9 and 0.17 ppm for carbon and proton data, respectively, were obtained.

Based on these evidences and on biogenetic considerations, the absolute configuration of compound **4** was deduced as 1*S*, *2S*, 5*S*, 9*R*, 12*S*, 26*S*, 27*R*, 30*R*, 31*S*, 33*S*, 35*S* as shown in Fig. 1.

Ximaolide L (**5**) was obtained as colorless oil. The HREI-MS at *m/z* 714.4318 $[M]^+$ (calcd. for $C_{41}H_{62}O_{10}$, 714.4343) indicated the molecular formula as $C_{41}H_{62}O_{10}$. Its ^{1}H and ^{13}C NMR data (Tables 1 and 2) were extremely similar to those of co-isolated ximaolide A (**6**). In fact, the only difference between **5** and **6** was the presence of a peroxide at the C-36 position of **5**, since the ^{13}C NMR signal of C-36 has been shifted from δ_C 33.0 (CH_2) in **6** to δ_C 86.6 (CH) in **5** and there are two additional oxygens in the composition of **5**. The obvious NOE correlations between the adjacent H-2 (δ_H 4.20) and H-36 (δ_H 4.68) on the cyclohexene ring B assigned the configuration of C-36. Moreover, thanks to ^{1}H NMR spectroscopic analysis, it is possible to observe a coupling constant between H-2 and H-36 ($^3J_{2,36}$ = 4.5 Hz) which suits better with the isomer configuration 36*R** (Fig. 6) as it is described in Karplus equation. Thus, the α-orientation of the peroxide group was determined. All the other configurations of **5** were determined to be the same as those of **6** by their similar NMR data around the

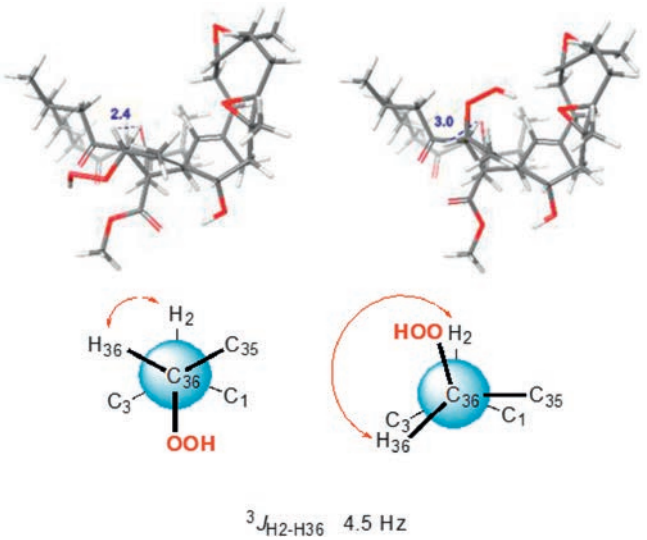

Fig. 6. The determination of the configuration at C-36 of **5**.

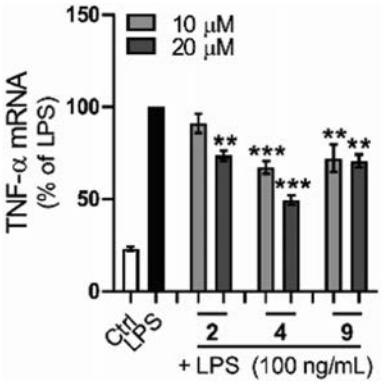

Fig. 7. Effects of the bioactive compounds **2**, **4** and **9** on LPS-induced inflammatory response in RAW264.7 macrophages. Results are expressed as mean ± SEM. $^{**}P < 0.01$, $^{***}P < 0.001$ *vs*. the LPS group μM: μmol/L.

chiral centers and similar CD spectra with the same positive Cotton effects at 282 nm.

In the biological activity test, the new compounds **1**–**5** gave negative results in both antibacterial and cytotoxic effects, whereas in the anti-inflammatory assay, ximaolides I (**2**), K (**4**), and F (**9**) exhibited significant inhibition of LPS-induced TNF-α protein release in RAW264.7 macrophages at a concentration of 20 μmol/L (Fig. 7). In addition, none of the compounds showed obvious cytotoxicity against RAW264.7 cells, with inhibition ratio less than 50% at a concentration of 40 μmol/L.

In summary, five new (**1**–**5**) and four known (**6**–**9**) biscembranoids were isolated and characterized from the Hainan soft coral *S. tortuosum* collected off Yalong Bay. Among them, compounds **1** and **2**, containning 1,35-bridged lactone moiety in ring B, and compound **5**, comprising a peroxide group, are unprecedented natural biscembranoids. The discovery of such novel structure skeleton has further expanded the chemical diversity and complexity of marine terpenoids, which was probably influenced by the different living environment of the title animals, since they were collected in a different water area as our previously reported ones [7,8]. It is worth mentioning that the determination of configuration is a big challange for cembranoids and biscembranoids, since NOESY experiments are not 100% reliable due to the conformation flexibility of the macrocyle in these compounds. The stereochemistry of the reported new compounds **1**–**5** were determined by a combination of NOESY experiments, QM-NMR calculations, ECD spectra comaprison, and biogenetic considerations. In the bioassay, it is suprising that the new compounds did not show cytotoxicity or antimicrobial activity as did the previouly reported analogs, while anti-inflammatory activity of the new compounds were observed, which may give an insight for related drug discovery.

Declaration of competing interest

The authors report no declarations of interest.

Acknowledgments

This research work was financially supported by the National Natural Science Foundation of China (NSFC, Nos. 81991521, 8202290170, 42076099), the NSFC/CNRS (Centre National de la Recherche Scientifique) Joint Project (No. 81811530284), the National Key Research and Development Program of China (No. 2018YFC0310903), and the SKLDR/SIMM Project (No. SIMM1903ZZ-04). X.-W. Li is also thankful for the Shanghai Rising-Star Program (No. 20QA1411100) and SA-SIBS Scholarship Program. We thank Prof. X.-B. Li from Hainan University for the taxonomic identification of the soft coral material.

Appendix A. Supplementary data

Supplementary material related to this article can be found, in the online version, at doi:https://doi.org/10.1016/j.cclet.2020.11.037.

References

[1] L.F. Liang, Y.W. Guo, Chem. Biodivers. 10 (2013) 2161–2196.
[2] P. Sun, F.Y. Cai, G. Lauro, et al., J. Nat. Prod. 82 (2019) 1264–1273.
[3] W. Li, Y.H. Zou, M.X. Ge, et al., Mar. Drugs 15 (2017) 85.
[4] P. Sun, Q. Yu, J. Li, et al., J. Nat. Prod. 79 (2016) 2552–2558.
[5] C.Y. Huang, P.J. Sung, C. Uvarani, et al., Sci. Rep. 5 (2015) 15624.
[6] H.N. Nguyen, P.T. Tung, N.T. Ngoc, et al., Chem. Pharm. Bull. 63 (2015) 636–640.
[7] R. Jia, Y.W. Guo, P. Chen, et al., J. Nat. Prod. 70 (2007) 1158–1166.
[8] R. Jia, Y.W. Guo, E. Mollo, et al., Helv. Chim. Acta 91 (2008) 2069–2074.
[9] T. Iwagawa, K. Hashimoto, H. Okamura, et al., J. Nat. Prod. 69 (2006) 1130–1133.
[10] R. Jia, T. Kurtán, A. Mándi, et al., J. Org. Chem. 78 (2013) 3113–3119.
[11] I.G. Rodrigues, M.G. Miguel, W. Mnif, Molecules 24 (2019) 781.
[12] M. Yang, X.L. Li, J.R. Wang, et al., J. Org. Chem. 84 (2019) 2568–2576.
[13] G. Li, H. Li, Q. Zhang, et al., J. Org. Chem. 84 (2019) 5091–5098.
[14] (a) F. Ye, J. Li, Y. Wu, et al., Org. Lett. 20 (2018) 2637–2640;
(b) F. Ye, Z.D. Zhu, J.S. Chen, et al., Org. Lett. 19 (2017) 4183–4186.
[15] S.W. Li, F. Ye, Z.D. Zhu, et al., Acta Pharm. Sin. B 8 (2018) 944–955.
[16] Q.H. Wu, S.W. Li, H. Xu, et al., Angew. Chem. Int. Ed. 59 (2020) 12105–12112.
[17] Y.F. Li, L.L. He, H.L. Liu, et al., J. Asian Nat. Prod. Res. 15 (2013) 566–573.
[18] P. Yan, Z. Deng, L. van Ofwegen, et al., Chem. Biodivers. 8 (2011) 1724–1734.
[19] L.M. Zeng, W.J. Lan, J.Y. Su, et al., J. Nat. Prod. 67 (2004) 1915–1918.
[20] T. Kurtán, R. Jia, Y. Li, et al., Eur. J. Org. Chem. 2012 (2012) 6722–6728.
[21] M.W. Lodewyk, M.R. Siebert, D.J. Tantillo, Chem. Rev. 112 (2012) 1839–1862.
[22] N. Grimblat, A.M. Sarotti, Chem. Eur. J. 22 (2016) 12246–12261.